Arnold Mathematical Journal (2021) 7:619–637
https://doi.org/10.1007/s40598-021-00188-6

RESEARCH CONTRIBUTION

New Invariants of Poncelet–Jacobi Bicentric Polygons

Pedro Roitman[1] · **Ronaldo Garcia**[2] · **Dan Reznik**[3]

Received: 22 March 2021 / Revised: 3 July 2021 / Accepted: 7 August 2021 /
Published online: 18 August 2021
© Institute for Mathematical Sciences (IMS), Stony Brook University, NY 2021

Abstract
The 1d family of Poncelet polygons interscribed between two circles is known as the Bicentric family. Using elliptic functions and Liouville's theorem, we show (i) that this family has invariant sum of internal angle cosines and (ii) that the pedal polygons with respect to the family's limiting points have invariant perimeter. Interestingly, both (i) and (ii) are also properties of elliptic billiard N-periodics. Furthermore, since the pedal polygons in (ii) are identical to inversions of elliptic billiard N-periodics with respect to a focus-centered circle, an important corollary is that (iii) elliptic billiard focus-inversive N-gons have constant perimeter. Interestingly, these also conserve their sum of cosines (except for the $N = 4$ case).

Keywords Poncelet · Jacobi · Elliptic functions · Porism · Elliptic billiards · Bicentric · Confocal · Polar · Inversion · Invariant

Mathematics Subject Classification 51M04 · 51N20 · 51N35 · 68T20

1 Introduction

The bicentric family is a 1d family of Poncelet N-gons interscribed between two specially chosen circles [19, Poncelet's Porism]. The special case of a family of triangles with fixed incircle and circumcircle was originally studied by Chapple 80 years before Poncelet [14]. Any pair of conics with at least two complex conjugate points of intersection can be sent to a pair of circles via a suitable projective transformation [2]. Based on this, in the 1820s, Jacobi produced an alternative proof to Poncelet's Great

✉ Dan Reznik
dreznik@gmail.com

1 Universidade de Brasìlia, Brasìlia, DF, Brazil

2 Universidade de Goiás, Goiânia, GO, Brazil

3 Data Science Consulting Ltd, Rio de Janeiro, RJ, Brazil

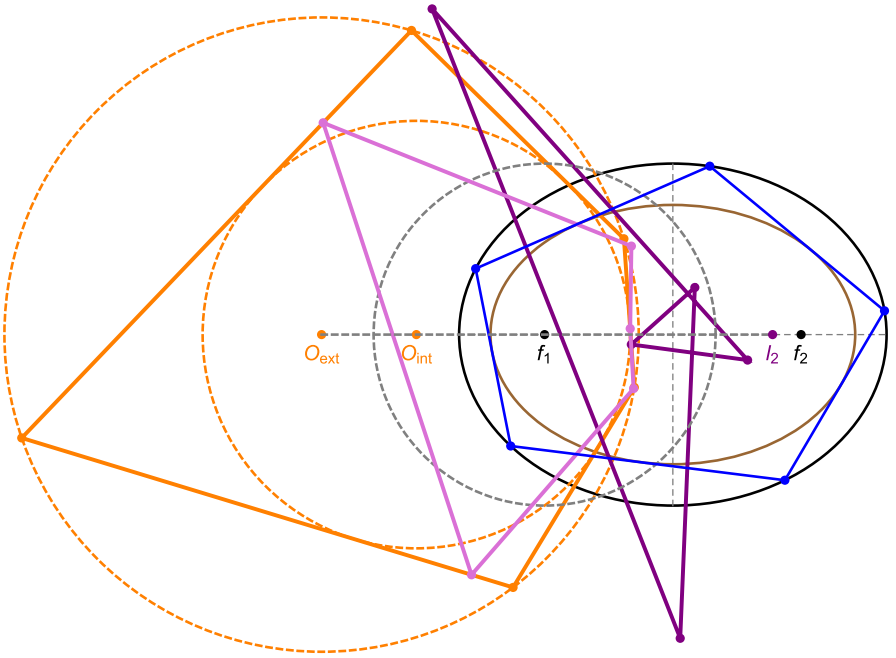

Fig. 1 The bicentric family (solid orange) is the polar image of elliptic billiard N-periodics (blue) with respect to a circle (dashed gray) centered on f_1 (which coincides with limiting point ℓ_1). Also shown are the constant-perimeter bicentric pedals (pink and purple) with respect to either limiting point, $f_1 = \ell_1$ and ℓ_2. Video (colour figure online)

theorem based on simplifications afforded by his elliptic functions over the bicentric family [5,7,13].

Referring to Fig. 1, a known fact is that the *polar image*[1] of two non-intersecting circles with respect to either one of their *limiting points* is a pair of confocal conics with a focus coinciding with the limiting point chosen [2] (see Appendix A).

Recall that a pair of non-intersecting circles $\mathcal{C}_1$ and $\mathcal{C}_2$ is associated with a pair of *limiting points* ℓ_1, ℓ_2 which, if taken as centers of inversion,[2] send the original circles to two distinct pairs of concentric circles [19, Limiting Points].

Conversely, the bicentric family is the polar image of elliptic (or hyperbolic) billiard N-periodics with respect to a circle centered on a focus (see Sect. 5). Recall the latter conserve both perimeter[3] and Joachimsthal's constant [18].

Main Results Though the bicentric family was much studied in the last 200 years, interactive experimentation with their dynamic geometry has led us to detect and

[1] The polar of a point P with respect to a circle $\mathcal{C}$ centered on O is the line L containing the inversion of P wrt $\mathcal{C}$ and perpendicular to OP.

[2] Note that ℓ_1, ℓ_2 coincide with the two points of intersection of all circles orthogonal to $\mathcal{C}_1$ and $\mathcal{C}_2$. This implies that the abovementioned inversions will result in concentric circles.

[3] Billiard inscribed in hyperbolas conserve *signed* perimeter, see Sect. 5.

prove a few new curious facts, perhaps known to the giants of the nineteenth century but never jotted down.

- Theorem 1: The sum of the cosines of bicentric polygons is invariant over the family. This mirrors an invariant recently proved for elliptic billiard N-periodics [1,4,10,16].
- Theorem 2 The perimeter of pedal polygons of the bicentrics with respect to its limiting points is invariant; see Fig. 1. Notice this too mirrors perimeter invariance of elliptic billiard N-periodics.
- Corollary 1: bicentric pedals with respect to a limiting point are identical to the inversion of billiard N-periodics with respect to a focus; therefore, the latter also conserves perimeter. In fact, it was this surprising observation (see this Video) that prompted the current article.
- Conjecture 1: Experiments show that the two limiting pedal polygons also conserve their sum of cosines, except for the case of the $N = 4$ pedal with respect to ℓ_1.

Article Structure

In Sect. 2, we review Jacobi's parametrization for bicentric polygons. We then use it to obtain expressions in terms of Jacobi elliptic functions for each of the above invariants, see Sects. 3 and 4. Section 5 paints a unified view of the five polygon families mentioned herein. A list of illustrative videos appear in Sect. 6.

Details of polar and pedal transformations are covered in Appendix A. The parameters for a pair of confocal ellipses (or hyperbolas) which are the polar image of the bicentric pair are given in Appendix B. Conversely, the parameters for a bicentric pair which is the polar image of confocal ellipses are given in Appendix C. In Appendix D, we provide elementary parametrizations for the vertices of $N = 3$ and $N = 4$ bicentric polygons. In Appendix E, we provide explicit expressions of their perimeters and sums of cosines as well as curious properties thereof.

Related Work

A few of our experimental conjectures for elliptic billiard N-periodic invariants [10,16] have been proved: (i) invariant sum of cosines and (ii) invariant product of outer polygon cosines [1,4], and (iii) invariant outer-to-orbit area ratio (for odd N) [6]. Dozens of other conjectured invariants appear in [17].

2 Review: Jacobi's Parametrization for Bicentric Polygons

In 1828, Jacobi found a beautiful proof for a special case of Poncelet's closure theorem using elliptic functions. In particular, he provided a very simple parametrization for the family of N-sided bicentric polygons that appear in Poncelet's theorem. We will use his parametrization below, and it is appropriate to recall it here.

Referring to Fig. 2, consider two circles $\mathcal{C}_R$ and $\mathcal{C}_r$, with radii R and r, respectively. Let d denote the distance between their centers. We will consider polygons that are

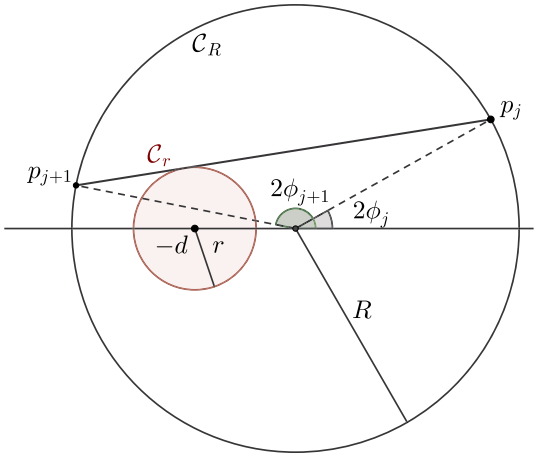

Fig. 2 A pair of circles, along with a chord p_j, p_{j+1} of the outer circle tangent to the inner one

inscribed in $\mathcal{C}_R$ and also are either inscribed or exscribed in $\mathcal{C}_r$. By exscribed in $\mathcal{C}_r$, we mean that extensions of the sides of the polygon are tangent to $\mathcal{C}_r$. Let $p_j(u)$, $j = 1, \ldots, N$ be the vertices of a N-sided bicentric family of polygons, parametrized by the real variable u, with all the vertices in $\mathcal{C}_R$.

Jacobi noticed that his elliptic functions could be used to provide an explicit expression for the $p_j(u)$. Namely, if we write

$$p_j(u) = R\left[\cos\left(2\phi_j(u)\right), \sin\left(2\phi_j(u)\right)\right]. \tag{1}$$

Indeed, he proved that [5]:

$$\phi_j(u) = \mathrm{am}(u + j\sigma, k), \tag{2}$$

where $\mathrm{am}(u, k)$ is the classical Jacobi amplitude function [3], k is the modulus and it is related to R, r and d by the following expression [5, pp. 315]:

$$k^2 = \frac{4Rd}{(R+d)^2 - r^2}, \quad 0 < k < 1. \tag{3}$$

The real number K is defined by:

$$K = \int_0^{\frac{\pi}{2}} \frac{\mathrm{d}t}{\sqrt{1 - k^2 \sin^2 t}},$$

and finally, σ is given by

$$\sigma = \frac{4\tau K}{N},$$

where τ is a positive integer and $N > 2$.

Actually, Jacobi treated only the case where one of the circles is inscribed, but his argument also holds for the exscribed case [5].

Below we recall some fundamental facts about three of Jacobi's elliptic functions: $sn(z,k) = \sin(\mathrm{am}(z,k))$, $cn(z,k) = \cos(\mathrm{am}(z,k))$ and $dn(z,k) = \sqrt{1-k^2 sn^2(z,k)}$, where $z \in \mathbb{C}$, and $0 < k < 1$ is the elliptic modulus. Since k is fixed, we write $sn(z)$ instead of $sn(z,k)$, etc.

These functions have two independent periods and also have simple poles at the same points. In fact:

$$\begin{aligned} sn(u+4K) &= sn(u+2iK') = sn(u), \\ cn(u+4K) &= cn(u+2K+2iK') = cn(u), \\ dn(u+2K) &= dn(u+4iK') = dn(u), \\ K' &= K(k'), \quad k' = \sqrt{1-k^2}. \end{aligned}$$

The poles of these three functions, which are simple, occur at the points

$$2mK + i(2n+1)K', \quad m, n \in \mathbb{Z}.$$

They also display a certain symmetry around the poles. Namely, if z_p is a pole of $sn(z)$, $cn(z)$ and $dn(z)$, then, for every $w \in \mathbb{C}$, we have [3, Chapter 2]:

$$\begin{aligned} sn(z_p + w) &= -\,sn(z_p - w), \\ cn(z_p + w) &= -\,cn(z_p - w), \\ dn(z_p + w) &= -\,dn(z_p - w). \end{aligned} \tag{4}$$

3 Bicentric Family: Invariant Sum of Cosines

Theorem 1 *The sum of cosines of angles internal to the family of N-periodics inscribed in a bicentric pair is invariant.*

Proof Let $\{p_j(u)\}$, as in (1), denote the vertices of the family of bicentric polygons. Let $\theta_j(u)$ denote the internal angle at the vertex $p_j(u)$. It follows from elementary geometry that $\cos\theta_j(u) = -\cos(\phi_{j+1}(u) - \phi_{j-1}(u))$. Thus, if we denote by $S(u)$ the sum of the cosines of the internal angles, we have:

$$S(u) = \sum \cos\theta_j(u) = -\sum \big(cn(u_{j+1})cn(u_{j-1}) + sn(u_{j+1})sn(u_{j-1})\big), \tag{5}$$

where $u_j = u + j\sigma$.

We now consider the natural complexified version of $S(u)$ defined on the complex plane by assuming that u is a complex variable. To prove that S is constant, it is sufficient to show that it has no poles and then apply Liouville's theorem.

So, suppose that $u = u_p$ is a pole of S. This implies that, for a certain index j, $u_j = u_p + j\sigma$ is a common pole of $cn(z)$ and $sn(z)$. We will now see that this leads to a contradiction.

In fact, by looking at (5), the terms where u_j appears are given by

$$-(cn(u_j)cn(u_{j-2}) + sn(u_j)sn(u_{j-2}) + cn(u_{j+2})cn(u_j) + sn(u_{j+2})sn(u_j)).$$

Thus, the coefficients of $cn(u_j)$ and $sn(u_j)$ are, respectively:

$$-(cn(u_{j-2}) + cn(u_{j+2})),$$
$$-(sn(u_{j-2}) + sn(u_{j+2})).$$

Note that by (4) both coefficients are zero, and they cancel out the simple poles of $cn(z)$ and $sn(z)$ at u_j, so u_p is not a pole of S. □

4 Bicentric Limiting Pedals: Invariant Perimeter

In this section, we prove that the two pedal polygons of a bicentric Poncelet family with respect to circles centered on either of its two *limiting points* (see below) conserve perimeter.

Definition 1 (*Pedal polygon*) Given a planar polygon $\mathcal{P}$ and a point p, the *pedal polygon* $\mathcal{P}_\perp$ of $\mathcal{P}$ wrt p has vertices q_j at the orthogonal projections of p onto the jth sideline $p_j p_{j+1}$ or extension thereof.

Definition 2 (*Limiting point*) Any pair of non-intersecting circles is associated with a pair of "limiting" points ℓ_1, ℓ_2 which lie on the line connecting the centers, with respect to which the circles are inverted to a concentric pair.

Let $\mathcal{C}_R$ be a circle of radius R centered at the origin $(0, 0)$ and $\mathcal{C}_r$ be a circle of radius r centered at $(-d, 0)$. Then the limiting points $(\delta_\pm, 0)$ of the pencil of circles defined by $\mathcal{C}_R$ and $\mathcal{C}_r$ has abscissa given by [19, Limiting Point, Eqn. 5]:

$$\delta_\pm = \frac{r^2 - R^2 - d^2 \pm \sqrt{d^4 - 2(R^2 + r^2)d^2 + (R^2 - r^2)^2}}{2d}. \tag{6}$$

Let $\mathcal{P}(u)$ be the family of bicentric polygons with respect to a pair of circles C_R and C_r, where u is the real parameter introduced by Jacobi, with vertices given by (1). Let ℓ denote a limiting point of the pencil defined by these circles, as in (6). Below, we derive an expression for the length of the sides of pedal polygons $\mathcal{P}_\perp(u)$ defined by $\mathcal{P}(u)$ and ℓ.

Lemma 1 *Let $p_{j-1}(u)$, $p_j(u)$ and $p_{j+1}(u)$ be three consecutive vertices of $\mathcal{P}(u)$, let $s_j(u) = |q_{j+1}(u) - q_j(u)|$ be jth sidelength of $\mathcal{P}_\perp$. Then*:

$$s_j(u) = \frac{r_j(u)\rho_j(u)}{2R}, \tag{7}$$

where $r_j(u) = \left|p_{j-1}(u) - p_{j+1}(u)\right|$ *and* $\rho_j(u) = \left|\ell - p_j(u)\right|$. *In addition,* $r_j(u)$ *and* $\rho_j(u)$ *are given by the following expressions.*

$$\begin{aligned} r_j(u) &= 2R\sin\left(\phi_{j+1}(u) - \phi_{j-1}(u)\right) \\ &= 2R\left(sn(u_{j+1})cn(u_{j-1}) - sn(u_{j-1})cn(u_{j+1})\right), \end{aligned} \tag{8}$$

where $u_j = u + j\sigma$.

$$\rho_j(u) = \frac{2}{k}\sqrt{-\delta_\pm R}\; dn(u_j). \tag{9}$$

Proof The proof of (7) follows the standard one for sidelengths of the pedal triangle [12, pp. 135–141]. Equation (8) follows by inspection from Fig. 2, and the definition of Jacobi's $sn(u)$ and $cn(u)$. Finally, (9) is a long but simple computation. Below we show a few intermediate steps. First, if we let $\ell = (\delta_\pm, 0)$ be either limiting point. Then:

$$\rho_j(u) = \cos(\phi_j(u))\sqrt{R^2 - 2R\delta_\pm} + \delta_\pm^2.$$

It is straightforward to check that $\delta_\pm < 0$. Substitute the expression (6) for $\delta_\pm$ in the expression for $\rho_j(u)$ to obtain:

$$\rho_j(u) = \sqrt{\frac{-\delta_\pm}{d}\Big(R^2 + d^2 - r^2 - 2Rd\cos\left(2\phi_j(u)\right)\Big)}.$$

Finally, using (3), we get:

$$\rho_j(u) = \frac{2}{k}\sqrt{-\delta_\pm R}\sqrt{1 - k^2 sn^2(u_j)} = \frac{2}{k}\sqrt{-\delta_\pm R}\; dn(u_j).$$

□

We are now in a position to prove the following.

Theorem 2 *The perimeters* $L_\pm$ *of the pedal polygons of the bicentric Poncelet family with respect to either limiting point are invariant.*

Proof From Lemma 1, the perimeter is given by:

$$L_\pm(u) = \frac{\sqrt{-\delta_\pm R}}{k}\sum dn(u_j)\Big(sn(u_{j+1})cn(u_{j-1}) - sn(u_{j-1})cn(u_{j+1})\Big).$$

To prove the above is constant, we consider its natural complexified version, that is, we think of $L_\pm$ as function of a complex variable u. Clearly, $L_\pm$ becomes a meromorphic function defined on the complex plane. To prove that $L_\pm$ is constant, we will show that it is entire and bounded. So, by Liouville's theorem, it must be constant.

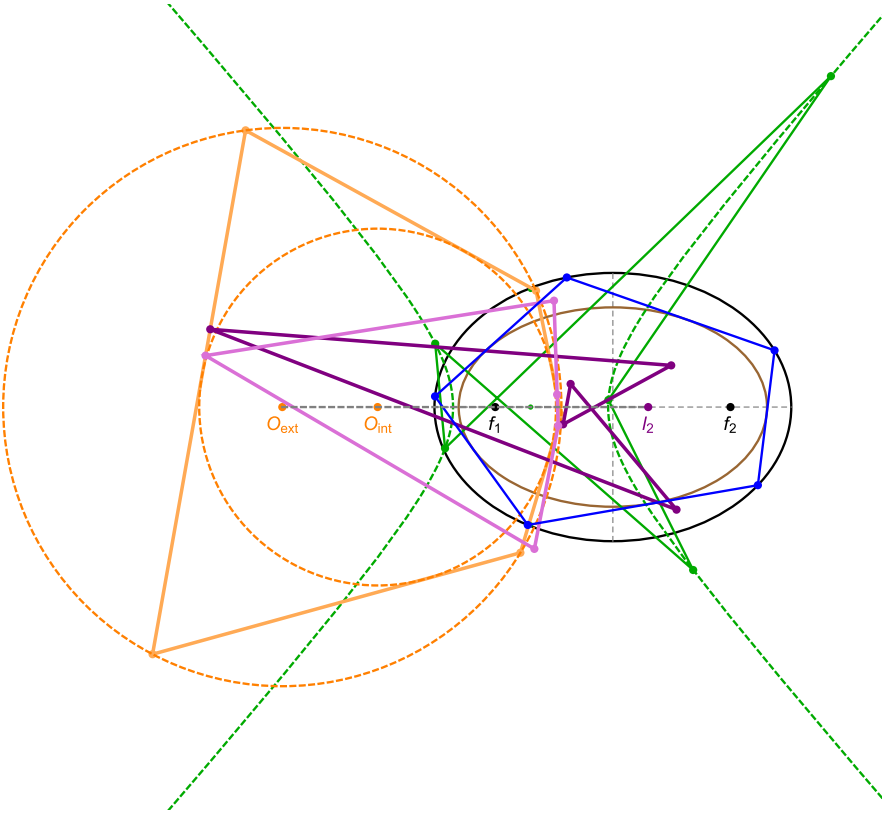

Fig. 3 The bicentric family (solid orange) and its two polar images: the elliptic billiard (blue) and the hyperbolic billiard (green). Also shown are the two pedal polygons (pink and purple) with respect to the limiting points $\ell_1 = f_1$ and ℓ_2. All but the bicentrics have constant perimeter. All five families conserve their sum of cosines (colour figure online)

In turn this amounts to showing $L_\pm$ has no poles. Now, suppose that, for $u = u_p$, a certain u_j is a common simple pole of $sn(z)$, $cn(z)$ and $dn(z)$. This is the only way that $L_\pm$ can have a pole.

From the expression of $L_\pm$, it follows there are three terms in the sum where the pole u_j of the three Jacobian elliptic functions appears:

$$\begin{aligned} &dn(u_{j-1})\left(sn(u_j)cn(u_{j-2}) - sn(u_{j-2})cn(u_j)\right), \\ &dn(u_j)\left(sn(u_{j+1})cn(u_{j-1}) - sn(u_{j-1})cn(u_{j+1})\right), \\ &dn(u_{j+1})\left(sn(u_{j+2})cn(u_j) - sn(u_j)cn(u_{j+2})\right). \end{aligned}$$

We have to prove that the sum of these terms is finite at u_j. To see this, consider first the term that multiplies $dn(u_j)$, namely

$$sn(u_{j+1})cn(u_{j-1}) - sn(u_{j-1})cn(u_{j+1}).$$

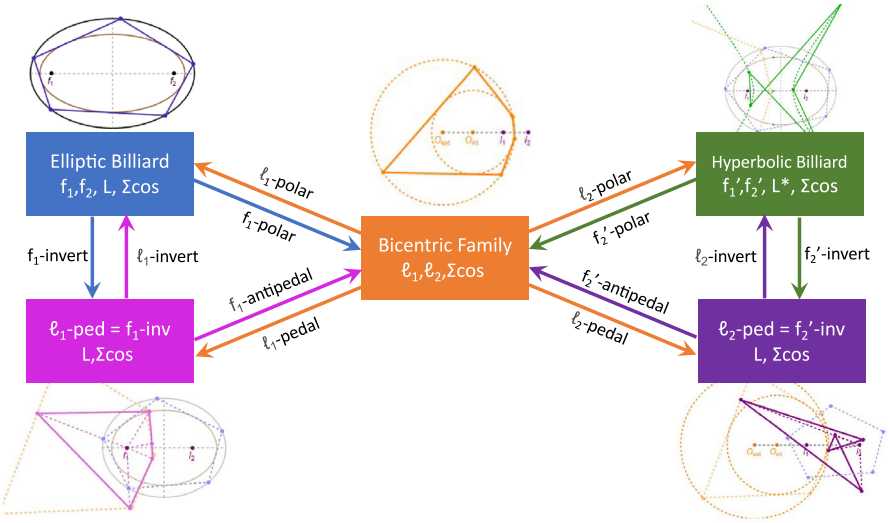

Fig. 4 The bicentric family (orange, center) is the hub from which four polygon families can be derived: the (i) elliptic (resp. (ii) hyperbolic) billiard with foci $f_1 = \ell_1$, f_2 (resp. f_1' and $f_2' = \ell_2$) is the bicentric polar image with respect to ℓ_1 (resp. ℓ_2); (iii) the first (resp. second) pedal is obtained with respect to ℓ_1 (resp. ℓ_2). These are the inversive image of the elliptic and hyperbolic billiards with respect to $l_1 = f_1$ or $l_2 = f_2'$, respectively. With the exception of the bicentrics, all 4 derived families conserve perimeter L (in the case of the hyperbolic billiard, it is the *signed* perimeter L^* which is conserved). All five families conserve sum of cosines, except for $N = 4$ ℓ_1-pedals (colour figure online)

Since $u_j = u + j\sigma$ is a pole and $u_{j+1} = u_j + \sigma, u_{j-1} = u_j - \sigma$ it follows from (4) that $sn(u_{j-1}) = -sn(u_{j+1})$ and $cn(u_{j-1}) = -cn(u_{j+1})$. Therefore, the expression above is zero. And this cancels the simple pole of $dn(u)$ at u_j. The same argument can be applied to the terms that multiply $sn(u_j)$ and $cn(u_j)$ and this shows that u_p is not a pole of $L_\pm$.

So $L_\pm$ has no poles and by the periodicity of the elliptic functions, it must be bounded. Thus, by Liouville's theorem $L_\pm$ is constant. □

In Appendices B and C we show that the image of two nested circles wrt to ℓ_1 is a confocal pair of ellipses; therefore under this transformation, a bicentric N-gon is sent to an elliptic billiard N-gon. Lemmas 2 and 3 found in the Appendix A show that the bicentric pedal with respect to ℓ_1 is identical to its polar image (elliptic billiard N-periodic) inverted with respect to a circle centered on $f_1 = \ell_1$. Therefore:

Corollary 1 *Over the family of N-periodics in the elliptic billiard* (*confocal pair*), *the perimeter of inversions of said N-periodics with respect to a focus-centered circle is invariant.*

Though not yet proved, experimental evidence suggests:

Conjecture 1 *The sum of cosines of bicentric pedal polygons with respect to either limiting point is invariant, except for the ℓ_1-pedal in the $N = 4$ case.*

5 A Tale of Five Polygons

Illustrated in Fig. 3 is the bicentric family along with its two limiting-pedals and its two polar images (elliptic and hyperbolic billiards), each with respect to a limiting point. While N-periodics in the elliptic billiard conserve perimeter, their hyperbolic version conserve *signed* perimeter, i.e., the length of a trajectory segment touching both hyperbola branches (resp. a single branch) is subtracted (resp. added) to the perimeter.

As shown in Fig. 4, the bicentric family can be regarded as a "hub" from which four derived polygon families can be obtained, all of which conserve both (signed) perimeter and the sum of cosines. Bicentric polygons themselves have variable perimeter.

6 List of Videos

Videos illustrating some of the above phenomena are listed on Table 1.

Acknowledgements We would like to thank Arseniy Akopyan, Sergei Tabachnikov, and Jair Koiller for invaluable discussions during the discovery phase. The second author is fellow of CNPq and coordinator of Project PRONEX/CNPq/FAPEG 2017 10 26 7000 508.

Appendix A: Polar Pedal Transformations

We review properties of polar and pedal transformations. A detailed treatment is found in [2,11].

In the discussion that follows, all geometric objects are contained in a fixed plane. Let $\mathcal{C}$ be a circle centered at f_1. The polar transformation with respect to $\mathcal{C}$ maps each straight line not passing through f_1 into a point, and maps each point different from f_1 into a straight line. This is done in the following manner.

Let $p \neq f_1$ be a point and let $p^\dagger$ be the inversion of p with respect to $\mathcal{C}$. The straight line L_p that passes through $p^\dagger$ and is orthogonal to the line joining p and $p^\dagger$ is the polar of p with respect to $\mathcal{C}$. Conversely, a line L not passing through f_1 has a point q as its pole with respect to $\mathcal{C}$ if $L = L_q$.

For a smooth curve γ not passing through f_1, we can define the polar curve $\gamma^\star$ in two equivalent ways. Let p be a point of γ and $T_p\gamma$ the tangent line to γ at p, we define $p^\star = (T_p\gamma)^\star$, and $\gamma^\star$ is the curve generated by $p^\star$ as p varies along γ. We can also think of $\gamma^\star$ as the curve that is the envelope of the 1-parameter family of lines L_p, where p is a point of γ.

The notion of a polar curve can be naturally extended to polygons in the following manner: let L_j, $j = 1, 2, \ldots, N$ be the consecutive sides of a planar polygon $\mathcal{P}$, and let q_j be the corresponding poles, then this indexed set of points are the vertices of what we call the polar polygon $\mathcal{P}^\star$. Alternatively, we can consider the polars of vertices of $\mathcal{P}$, and their consecutive intersections do define the vertices of $\mathcal{P}^\star$.

Although the next results are certainly classical, we could not find them explicitly in the literature, so we include them for the reader's convenience.

Table 1 Videos illustrating some phenomena presented herein

id	N	Title	**youtu.be/** < . >
01	5	Invariant-perimeter limiting point pedals	8m21fCz8eX4
02	3…8	Bicentric pedals, polars, and inversions I	jhXDKRFLpVk
03	3…8	Bicentric pedals, polars, and inversions II	A7F3szW7rUE
04	3…8	Bicentric pedals, polars, and inversions III	6TmaezNFrOs
05	4	Bicentric pedals, polars, and inversions IV	fZe6elRTfeA
06	5	A rose in the elliptic garden: the invariant-perimeter, focus-inversive family	wkstGKq5jOo
07	5	Focus-inversive polygons of elliptic Billiard self-intersected 5-periodics	LuLtbwkfSbc
08	5	Inversive arcs of elliptic billiard N-periodic segments and the bicentric family	mXkk_4RYrnU
09	6	Focus-inversive polygons of elliptic Billiard self-intersected 6-periodics	7lXwjXj-8YY
10	7	Focus-inversive polygons of elliptic billiard self-intersected 7-periodics I	BRQ39O9ogNE
11	7	Focus-inversive polygons of elliptic billiard self-intersected 7-periodics II	gf_aHyvbqOY
12	8	Focus-inversive polygons of elliptic billiard self-intersected 8-periodics I	5Lt9atsZhRs
13	8	Focus-inversive polygons of elliptic billiard self-intersected 8-periodics II	93xpGnDxyi0
14*	5	Circular loci of focus-inversive centroids of elliptic billiard simple 5-periodics	jzW84ZZApA
15*	5	Circular loci of focus-inversive centroids of elliptic billiard self-intersected 5-periodics	7bzID9SVwqM
16*	6	Focus-inversive polygons of elliptic billiard 6-periodics and the null-area antipedal polygon	fOAES-CzjNI
17*	5	Invariant area ratio of focus-inversives to elliptic billiard N-periodics	eG4UCgMkKl8
18*	5	Invariant product of areas amongst the two focus-inversive elliptic billiard N-periodics (odd N)	bTkbdEPNUOY

The last column is clickable and provides the YouTube code. The entries whose id has an asterisk (*) represent phenomena detected experimentally but not yet proved

Lemma 2 *Let $\mathcal{E}$ be an ellipse and f_1 one its the foci. Then the polar curve $\mathcal{E}^\star$ with respect to a circle $\mathcal{C}$ centered at f_1 is a circle. Let $\mathcal{H}$ be a hyperbola and f_1 one of its foci. Then, the polar curve $\mathcal{H}^\star$ with respect to a circle $\mathcal{C}$ centered at f_1 is a circle minus two points.*

Proof We will use polar coordinates for our computations. Without loss of generality, let $f_1 = (0, 0)$ and consider the parametrized conic given by:

$$\gamma(t) = \left[\frac{a(1-e^2)}{1+e\cos t}\cos t,\ \frac{a(1-e^2)}{1+e\cos t}\sin t\right],$$

where if $e > 1$, the trace of γ is a hyperbola and if $e < 1$, the trace of γ is an ellipse. The expression for the polar curve $\gamma^\star(t)$ is obtained by direct computation: compute the unit normal $\mathbf{n}(t)$ to $\gamma(t)$, and the distance $d(t)$ from the tangent line through $\gamma(t)$ to f_1. This yields:

$$\gamma^\star(t) = \left[\frac{e + \cos t}{a(1-e^2)}, \frac{\sin t}{a(1-e^2)}\right],$$

whose trace is clearly contained in a circle. For the hyperbola, the parameter t is such that $1 + e\cos(t) \neq 0$, this is why $\mathcal{H}^\star$ is a circle minus two points. □

Lemma 3 *Let $\mathcal{E}_1$ and $\mathcal{E}_2$ be two confocal ellipses and $\mathcal{E}_1^\star$ and $\mathcal{E}_2^\star$ be the circles as in Lemma 2, then f_1 is a limiting point of the pencil of circles defined by $\mathcal{E}_1^\star$ and $\mathcal{E}_2^\star$. In a similar way, let $\mathcal{E}$ and $\mathcal{H}$ be respectively an ellipse and hyperbola that are confocal, and let $\mathcal{E}^\star$ and $\mathcal{H}^\star$ be the circle and the circle minus 2 points, as in Lemma 2, then f_1 is a limiting point of the pencil of circles defined by $\mathcal{E}^\star$ and the circle that contains $\mathcal{H}^\star$.*

Proof Given two circles $\mathcal{C}_1$ and $\mathcal{C}_2$, a classical result states that the limiting points $\delta_\pm$ of the pencil of circles determined by $\mathcal{C}_1$ and $\mathcal{C}_2$ are such that the inversion of $\mathcal{C}_1$ and $\mathcal{C}_2$ with respect to circles centered on $\delta_\pm$ are concentric.

If we denote by a_i and e_i, $i = 1, 2$, respectively, the semi-major diameter and eccentricity of the ellipses $\mathcal{E}_1$ and $\mathcal{E}_2$, then, by symmetry, we can define an unknown limiting point as $\delta_p = (x, 0)$, and the concentric circle condition then becomes a quadratic equation in the variable x, where the coefficients depend on a_1, a_2, e_1 and e_2. Using the fact that $\mathcal{E}_1$ and $\mathcal{E}_2$ are confocal, which is equivalent to $e_1 a_1 = e_2 a_2$, and with some algebraic manipulations, the quadratic equation can be written as:

$$(a_1 - a_2)(a_1 + a_2)(e_2 a_2 x + 1) = 0,$$

so $f_1 = (0, 0)$ is indeed one of the limiting points of the pencil of circles. □

Appendix B: Polar Image of Bicentric Pair

Consider the pair of nested circles:

$$\mathcal{C}_{\text{int}} : \; x^2 + y^2 = r^2, \quad \mathcal{C}_{\text{ext}} : \; (x+d)^2 + y^2 = R^2.$$

Their limiting points ℓ_1 and ℓ_2 are given by [19, Limiting Points]:

$$\ell_1 = (R^2 - d^2 - r^2 - \Delta)/(2d), \quad \ell_2 = (R^2 - d^2 - r^2 + \Delta)/(2d),$$

where

$$\Delta = \sqrt{(d + R + r)\,(R - d + r)\,(R + d - r)\,(R - d - r)}.$$

Notice ℓ_1 (resp. ℓ_2) is internal (resp. external) to the circle pair. Below we show that the polar image of the $\mathcal{C}_{\text{int}}, \mathcal{C}_{\text{ext}}$ pair with respect to a circle of radius ρ centered on ℓ_1 (resp. ℓ_2) is a confocal pair of ellipses (resp. hyperbolas).

Lemma 4 *The polar image of $\mathcal{C}_{\text{int}}$ with respect to ℓ_1 is the ellipse $\mathcal{E}$ centered at*

$$\mathcal{O}_e = \left[\rho^2 \frac{d}{\Delta} + \frac{k-\Delta}{2d}, 0\right],$$

where $k = R^2 - d^2 - r^2$. Its semi-axes are given by:

$$a^2 = \rho^4 \left(\frac{2d^2r^2 + \Delta(k+\Delta)}{2\Delta^2 r^2}\right), \quad b^2 = \rho^4 \left(\frac{k+\Delta}{2\Delta r^2}\right).$$

Note that $c^2 = a^2 - b^2 = \rho^4 d^2/\Delta^2$.

Lemma 5 *The polar image of $\mathcal{C}_{\text{ext}}$ with respect to ℓ_1 is an ellipse $\mathcal{E}'$ confocal with $\mathcal{E}$ with semi-axes given by*:

$$a'^2 = \rho^4 \frac{(2R^2d^2 + \Delta(k'+\Delta))}{2\Delta^2 R^2}, \quad b'^2 = \rho^4 \left(\frac{k'+\Delta}{2\Delta R^2}\right),$$

where $k' = R^2 + d^2 - r^2$.

Lemma 6 *The polar image of $\mathcal{C}_{\text{int}}$ with respect to ℓ_2 is the hyperbola $\mathcal{H}$ centered at*

$$\mathcal{O}_h = \left[-\rho^2 \frac{d}{\Delta} + \frac{k+\Delta}{2d}, 0\right],$$

with semi-axes given by:

$$a_h^2 = \rho^4 \left(\frac{2d^2r^2 - \Delta(k-\Delta)}{2\Delta^2 r^2}\right), \quad b_h^2 = \rho^4 \left(\frac{k-\Delta}{2\Delta r^2}\right).$$

Note that $c_h^2 = a_h^2 + b_h^2 = \rho^4 d^2/\Delta^2$. Note also that $c = c_h$.

Lemma 7 *The polar image of $\mathcal{C}_{\text{out}}$ with respect to ℓ_2 is a hyperbola $\mathcal{H}'$ confocal with $\mathcal{H}$. Its semi-axes are given by*:

$$a_h'^2 = \rho^4 \left(\frac{2R^2d^2 - \Delta(k'-\Delta)}{2\Delta^2 R^2}\right), \quad b_h'^2 = \rho^4 \left(\frac{k'-\Delta}{2\Delta R^2}.\right)$$

Appendix C: Polar Image of Confocal Pair

Consider a pair of origin-centered confocal ellipses $\mathcal{E}$ and $\mathcal{E}'$ with semi-axes a, b and a', b', respectively. Their common foci f_1, f_2 lie at:

$$f_1 = [-c, 0], \quad f_2 = [c, 0],$$

where $c^2 = a^2 - b^2$.

Below we show that the polar image of the $\mathcal{E}, \mathcal{E}'$ pair with respect to a circle of radius ρ centered on f_1 is a pair of nested circles $\mathcal{C}_{\text{int}}, \mathcal{C}_{\text{ext}}$ with centers given by:

$$\mathcal{O}_{\text{int}} = \left[-c - \rho^2 \frac{c}{b^2}, 0\right], \quad \mathcal{O}_{\text{ext}} = \left[-c - \rho^2 \frac{c}{b'^2}, 0\right].$$

Note the distance d between said centers is given by:

$$d = \rho^2 \frac{c\,(a^2 - a'^2)}{b^2\, b'^2} = \rho^2 \frac{c a^2 J^2}{b'^2},$$

where $J = \sqrt{a^2 - a'^2}/(ab)$.

Their respective radii r, R are given by:

$$r = \rho^2 \frac{a}{b^2}, \quad R = \rho^2 \frac{a'}{b'^2}.$$

Let ℓ_1 (resp. ℓ_2) be the limiting point internal (resp. external) to $\mathcal{C}_{\text{int}}, \mathcal{C}_{\text{ext}}$.

Lemma 8 *The limiting points ℓ_1, ℓ_2 are given by*: $[-c, 0]$ *and* $[-c + \frac{\rho^2}{c}, 0]$.

Appendix D: Bicentric Vertices: $N = 3, 4$

Consider a pair of circles

$$\mathcal{C}_1 : x^2 + y^2 - r^2 = 0, \quad \mathcal{C}_2 : (x + d)^2 + y^2 - R^2 = 0.$$

D.1. $N = 3$

Let $(x_0, y_0) = (r \cos t, r \sin t) \in \mathcal{C}_1$. Let $d^2 = R(R - 2r)$. Then, the 3-periodic orbit is parametrized by $\{P_1, P_2, P_3\}$, where

$$P_1 = \left[\frac{\cos t(2\,d\,R\cos t + R^2 - d^2) + \Delta\,\sin t}{2\,R} - d, \frac{\sin t(2d\,R\,\cos t + R^2 - d^2) - \Delta\,\cos t}{2\,R}\right],$$

$$P_2 = \left[\frac{\cos t(2\,d\,R\cos t + R^2 - d^2) - \Delta\,\sin t}{2\,R} - d, \frac{\sin t(2d\,R\,\cos t + R^2 - d^2) + \Delta\,\cos t}{2\,R}\right],$$

$$P_3 = \left[-\frac{(R\cos t - d)\left(R^2 - d^2\right)}{R^2 + d^2 - 2\,dR\cos t}, \frac{-R\left(R^2 - d^2\right)\sin t}{R^2 + d^2 - 2\,dR\cos t} \right],$$
$$\Delta = \sqrt{\left(R^2 + d^2 - 2dR\,\cos t\right)\left(3\,R^2 - d^2 + 2\,dR\cos t\right)}.$$

Under the above pair of circles, the limiting points are at:

$$l_1 = \left[\frac{R^2 - d^2}{8\,dR^2}\left(\sqrt{(9\,R^2 - d^2)(R^2 - d^2)} + 3\,R^2 + d^2\right), 0 \right],$$
$$l_2 = l_1 - \left[\frac{\sqrt{9R^2 - d^2}(R^2 - d^2)^{\frac{3}{2}}}{4R^2 d}, 0 \right].$$

D.2. $N = 4$

Let $(x_0, y_0) \in \mathcal{C}_1$. The Cayley condition for a pair of circles to admit Poncelet 4-periodics due to Kerawala is [19, Poncelet's Porism, Eq. 39]:

$$\frac{1}{(R-d)^2} + \frac{1}{(R+d)^2} - \frac{1}{r^2} = 0.$$

Let $P_i = [x_i, y_i]$, $i = 1, \ldots, 4$ denote the vertices of a bicentric 4-periodic. Let $\alpha = R^2 + d^2$ and $\beta = R^2 - d^2$. The vertices are parametrized as:

$$x_1 = \Delta\, y_0 - \frac{(\beta + 2\,dx_0)\,(d\alpha - \beta x_0)}{2\,\alpha},$$
$$y_1 = -\Delta\, x_0 + \frac{\left(2\,d\beta x_0 + \alpha^2\right) y_0}{2\,\alpha},$$
$$x_2 = -\Delta\, y_0 - \frac{(\beta + 2\,dx_0)\,(d\beta - \beta x_0)}{2\,\alpha},$$
$$y_2 = \Delta\, x_0 + \frac{2\,d\beta y_0\, x_0 + \alpha^2 y_0}{2\,\alpha},$$
$$x_3 = \frac{(((x_0^2\alpha\beta - 4x_0^2\alpha^2 + 3/2\beta^3 - 2\beta^2\alpha)\sqrt{2\alpha - 2\beta} + \beta(2\Delta\alpha y_0 + 8\alpha^2 x_0 - 8\alpha\beta x_0 + \beta^2 x_0))\beta)}{(4(\sqrt{2\alpha - 2\beta}\alpha x_0 + \beta(\beta - 2\alpha)/2)^2)},$$
$$y_3 = \frac{\alpha\beta(\alpha(2x_0 y_0\alpha + \beta(x_0 y_0 - 2\Delta))\sqrt{2\alpha - 2\beta} + (4\Delta x_0 - 2\beta y_0)\alpha^2 - 2\Delta\alpha\beta x_0 + \beta^3 y_0)}{(2\sqrt{2\alpha - 2\beta}\alpha x_0 - 2\alpha\beta + \beta^2)^2},$$
$$x_4 = -\frac{(((x_0^2\alpha\beta - 4x_0^2\alpha^2 + 3/2\beta^3 - 2\beta^2\alpha)\sqrt{2\alpha - 2\beta} + \beta(-2\Delta\alpha y_0 + 8\alpha^2 x_0 - 8\alpha\beta x_0 + \beta^2 x_0))\beta)}{(4(\sqrt{2\alpha - 2\beta}\alpha x_0 + \beta(\beta - 2\alpha)/2)^2)},$$
$$y_4 = \frac{(\alpha(2x_0 y_0\alpha + \beta(x_0 y_0 + 2\Delta))\sqrt{2\alpha - 2\beta} + (-4\Delta x_0 - 2\beta y_0)\alpha^2 + 2\Delta\alpha\beta x_0 + \beta^3 y_0)\beta}{(2\sqrt{2\alpha - 2\beta}\alpha x_0 - 2\alpha\beta + \beta^2)^2},$$
$$\Delta = \frac{\sqrt{-2\sqrt{2\alpha - 2\beta}\,\alpha x_0\beta^2 - 2x_0^2\alpha^3 + 2x_0^2\alpha^2\beta + \alpha^2\beta^2 + \alpha\beta^3 - \beta^4}}{(2\alpha}.$$

Under the above pair of circles, the limiting points are at:

$$l_1 = \left[\frac{R^2 - d^2}{2d}, 0 \right], \quad l_2 = \left[\frac{d(R^2 - d^2)}{R^2 + d^2}, 0 \right].$$

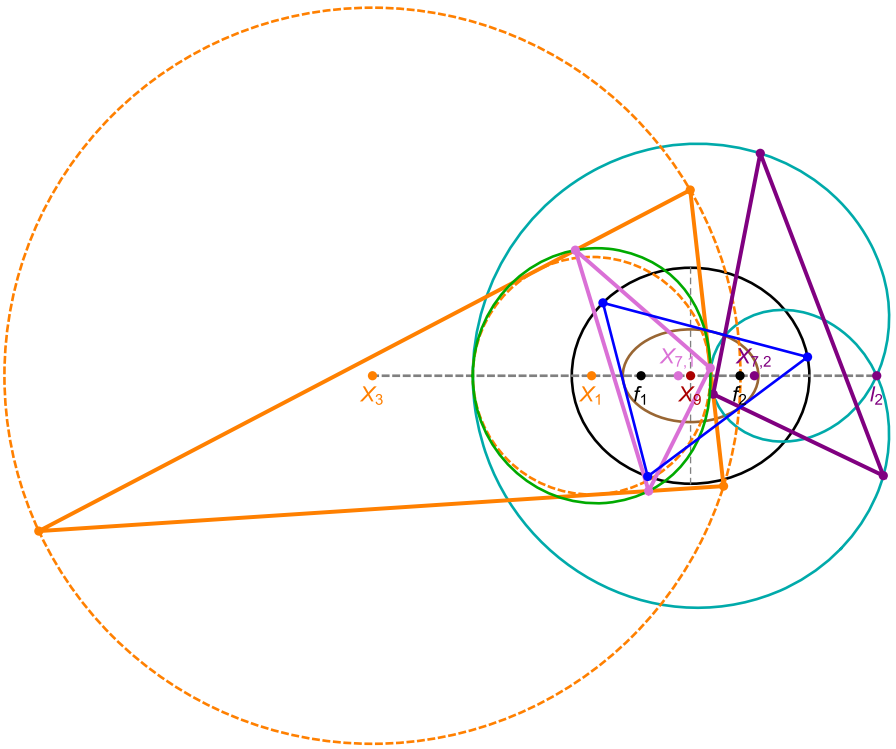

Fig. 5 $N = 3$ case: the bicentric family (solid orange) is the poristic family [8]. Its sum of cosines is invariant and equal to those of the two limit point pedals (pink and purple). The Gergonne points $X_{7,1}$ and $X_{7,2}$ of each pedal are stationary. (colour figure online) live

Appendix E: Limiting Pedal Perimeters for $N = 3$ and $N = 4$

Below we consider 3- and 4-periodics in the confocal pair where a, b are the semi-axes of the outer ellipse has axes (a, b). Below, set $\delta = \sqrt{a^4 - a^2b^2 + b^4}$ and $c^2 = a^2 - b^2$.

E.1. $N = 3$ case

Referring to Fig. 5, the perimeter $L^\dagger$ of the inversive polygon for the $N = 3$ family, originally derived in [15, Prop. 4] is given by:

$$L^\dagger = L_+ = \rho^2 \frac{\sqrt{\left(8\,a^4 + 4\,a^2b^2 + 2\,b^4\right)\delta + 8\,a^6 + 3\,a^2b^4 + 2\,b^6}}{a^2b^2}.$$

By Corollary 1, this is equal to the perimeter L_- of the bicentric pedal with respect to the focal limiting point.

$$L_- = \frac{\left(9\,R^2 - d^2\right)\left(R^2 - d^2\right)\sqrt{2}\rho^2}{16\,R^4 d} \sqrt{-\left(R^2 - d^2\right)^{\frac{3}{2}}\sqrt{9\,R^2 - d^2} + 3R^4 + 6R^2d^2 - d^4},$$

$$R = (2a^4 - 2a^2b^2 + b^4 + (2a^2 - b^2)\delta)a\rho^2/b^6, \quad d = (2a^2 - b^2 + 2\delta)c\rho^2a^2/b^6.$$

The perimeter L_+ of the bicentric pair with respect to the non-focal limiting point is given by:

$$L_+ = \frac{\left(9\,R^2 - d^2\right)\left(R^2 - d^2\right)\sqrt{2}\rho^2}{16\,R^4 d}\sqrt{\left(R^2 - d^2\right)^{\frac{3}{2}}\sqrt{9\,R^2 - d^2} + 3R^4 + 6R^2d^2 - d^4},$$
$$R = (2a^4 - 2a^2b^2 + b^4 + (2a^2 - b^2)\delta)a\rho^2/b^6, \quad d = (2a^2 - b^2 + 2\delta)c\rho^2a^2/b^6.$$

The sum of cosines of a triangle is given by $1 + r/R$ and is therefore constant for the $N = 3$ bicentric family. Let θ_i' denote the angles of the bicentric polygon. The sum of its cosines can be derived as:

$$\sum \cos\theta' = 1 + \frac{r}{R} = \frac{3R^2 - d^2}{2R^2}. \tag{10}$$

Proposition 1 *The sum of cosines for the first and second $N = 3$ bicentric pedals are constant and identical to* (10).

Note: In terms of the associated elliptic billiard parameters, this is given by [15, Prop. 6]:

$$\sum \cos\theta^{\dagger}{}_{(N=3)} = \frac{\delta(a^2 + c^2 - \delta)}{a^2c^2}.$$

Proof Using CAS, it follows from straightforward calculations with the orbit parametrized in Appendix D. □

The two limiting pedals have stationary Gergonne points X_7. The first one was derived in [9, Proposition 1]:

$$X_{7,1} = \left[c\left(1 - \frac{\rho^2}{\delta + c^2}\right), 0\right],$$
$$X_{7,1} = \frac{(R^2 - d^2)((R^2 - d^2)^{3/2}\sqrt{9R^2 - d^2} + 3R^4 + 6R^2d^2 - d^4)}{16R^4d}.$$

E.2. $N = 4$ case

Referring to Fig. 6, the perimeter $L^{\dagger}$ of the inversive polygon for billiard 4-periodics was originally derived in [9, Prop. 18]. It is identical to the perimeter of 4-periodics themselves and given by:

$$L^{\dagger} = L_{+,N=4} = \frac{4\sqrt{a^2 + b^2}}{b^2}. \tag{11}$$

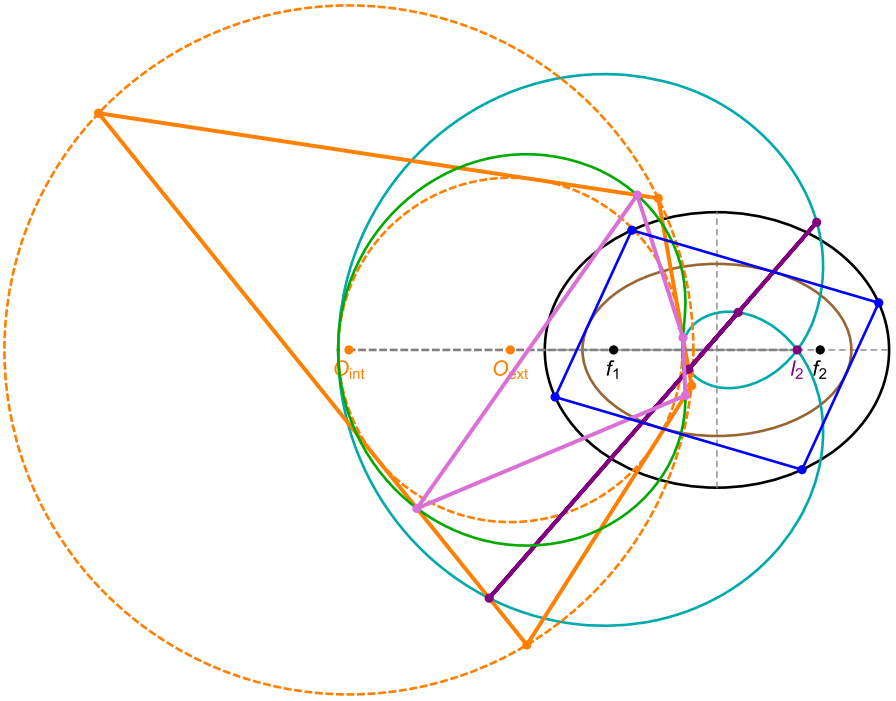

Fig. 6 In the $N = 4$ case, remarkable things happen: (i) the sum of cosines of the f_1-pedal (pink) is not constant; (iii) its perimeter is the same as the corresponding billiard 4-periodic; (iv) the vertices of the l_2-pedal (purple) are collinear and (v) the sum of its cosines is 4. (colour figure online) Video

Proposition 2 *In the $N = 4$ family, the vertices of the bicentric pedal with respect to the non-focal limiting point are collinear.*

Proof The polar image of the bicentric family with respect to ℓ_2 is a pair of confocal hyperbolas, see Appendix B, i.e., the polar image of bicentric 4-periodics is a billiard family. It can be shown its vertices are concyclic with the two hyperbolic foci f_1', f_2', one of which coincides with ℓ_2. Therefore, the inversion of said vertices with respect to ℓ_2 is a set of collinear points. □

As before, Eq. (11) is the same as the perimeter of the first bicentric pedal. The perimeter L_+ of the non-focal bicentric pedal is given by:

$$L_{-,N=4} = \frac{4a^2}{b^2 c}.$$

Regarding the sum of cosines, it is well known a circle-inscribed quadrilateral has supplementary opposing angles, i.e.:

Observation 1 *The sum of cosines of a bicentric $N = 4$ family is null.*

Since the second bicentric pedal is a degenerate polygon:

Observation 2 *The sum of cosines of the second limiting pedal to the* $N = 4$ *bicentric family is equal to* 4.

References

1. Akopyan, A., Schwartz, R., Tabachnikov, S.: Billiards in ellipses revisited. Eur. J. Math. (2020). https://doi.org/10.1007/s40879-020-00426-9
2. Akopyan, A.V., Zaslavsky, A.A.: Geometry of Conics. American Mathematical Society, Providence (2007)
3. Armitage, J.V., Eberlein, W.F.: Elliptic Functions. Cambridge University Press, London (2006)
4. Bialy, M., Tabachnikov, S.: Dan Reznik's identities and more. Eur. J. Math. (2020). https://doi.org/10.1007/s40879-020-00428-7
5. Bos, H.J.M., Kers, C., Raven, D.W.: Poncelet's closure theorem. Expo. Math. **5**, 289–364 (1987)
6. Chavez-Caliz, A.: More about areas and centers of Poncelet polygons. Arnold Math. J. (2020). https://doi.org/10.1007/s40598-020-00154-8
7. Dragović, V., Radnović, M.: Poncelet Porisms and Beyond: Integrable Billiards, Hyperelliptic Jacobians and Pencils of Quadrics. Frontiers in Mathematics. Springer, Basel (2011)
8. Gallatly, W.: The Modern Geometry of the Triangle. Francis Hodgson, London (1914)
9. Garcia, R., Reznik, D.: Invariants of self-intersected and inversive N-periodics in the elliptic billiard (2020). arXiv:2011.06640
10. Garcia, R., Reznik, D., Koiller, J.: New properties of triangular orbits in elliptic billiards. Am. Math. Mon. (2020) (**to appear**)
11. Glaeser, G., Stachel, H., Odehnal, B.: The Universe of Conics: From the Ancient Greeks to 21st Century Developments. Springer, Berlin (2016)
12. Johnson, R.A.: In: Young, J.W. (eds.) Advanced Euclidean Geometry, 2nd edn. Dover, New York (1960)
13. Nash, O.: Poring over Poncelet's porism (2018). http://bit.ly/3r1rwxv
14. Odehnal, B.: Poristic loci of triangle centers. J. Geom. Graph. **15**(1), 45–67 (2011)
15. Reznik, D., Garcia, R.: The talented Mr. inversive triangle in the elliptic billiard. Eur. J. Math. (2020) (**to appear**)
16. Reznik, D., Garcia, R., Koiller, J.: Can the elliptic billiard still surprise us? Math. Intell. **42**, 6–17 (2020). https://doi.org/10.1007/s00283-019-09951-2
17. Reznik, D., Garcia, R., Koiller, J.: Fifty new invariants of N-periodics in the elliptic billiard. Arnold Math. J. (2021). https://doi.org/10.1007/s40598-021-00174-y
18. Tabachnikov, S.: Geometry and Billiards. Student Mathematical Library, vol. 30. American Mathematical Society, Providence (2005)
19. Weisstein, E.: Mathworld. MathWorld—A Wolfram Web Resource (2019). http://mathworld.wolfram.com

Publisher's Note Springer Nature remains neutral with regard to jurisdictional claims in published maps and institutional affiliations.